SCIENTIFIC REPORTS

OPEN

SUBJECT AREAS:
STEROLS
METABOLIC DISORDERS
BIOMEDICAL MATERIALS
DRUG DELIVERY

Received
2 December 2013

Accepted
25 February 2014

Published
12 March 2014

Correspondence and requests for materials should be addressed to N.Y. (yui.org@tmd.ac.jp)

Lysosomal-specific Cholesterol Reduction by Biocleavable Polyrotaxanes for Ameliorating Niemann-Pick Type C Disease

Atsushi Tamura & Nobuhiko Yui

Department of Organic Biomaterials, Institute of Biomaterials and Bioengineering, Tokyo Medical and Dental University, 2-3-10 Kanda-Surugadai, Chiyoda, Tokyo 101-0062, Japan.

Niemann-Pick type C (NPC) disease is an autosomal recessive lysosomal trafficking disorder, in which the cholesterols are abnormally accumulated in lysosomes. Recently, the β-cyclodextrin (CD) derivatives are revealed to show therapeutic effect for NPC disease through the removal of accumulated cholesterols in lysosomes. Herein, to enhance the therapeutic effect and reduce the toxicity of β-CD derivatives, biocleavable Pluronic/β-CD-based polyrotaxanes (PRXs) bearing terminal disulfide linkages that can release threaded β-CDs in lysosomes were developed. The biocleavable PRXs show negligible interaction with the plasma membrane, leading to avoiding the toxicity of β-CDs derived from their hydrophobic cavity. Additionally, lysosomal release of threaded β-CDs from biocleavable PRXs by the intracellular cleavage of terminal disulfide linkages is found to achieve approximately 100-fold higher cholesterol removal ability from NPC disease-derived cells than β-CD derivatives. Consequently, the biocleavable PRXs is considered to be a noninvasive and effective therapeutics for NPC disease.

Lysosomal storage diseases are a family of intracellular metabolic diseases caused by defective function of lysosomal proteins[1]. Among them, Niemann-Pick type C (NPC) disease is an autosomal recessive lysosomal trafficking disorder caused by the dysfunction of either the NPC1 or NPC2 protein[2–4]; which induces the chronic accumulation of unesterified cholesterols and sphingolipids within late endosomes and lysosomes of cells throughout the body[2,3]. This abnormal cholesterol accumulation leads to various clinical symptoms, such as progressive neurodegeneration and hepatosplenomegaly, often resulting in fatality at an early age[2]. Nevertheless, there is currently no effective therapy for NPC disease, although various methodologies have been examined in attempt to establish NPC disease therapy[5–7]. Recently, hydroxypropyl-β-cyclodextrin (HP-β-CD), a derivative of cyclic oligosaccharide[8,9], has received tremendous attention as a potential therapeutic for NPC disease[10]. It has been revealed that HP-β-CD can reduce the lysosomal cholesterol content in NPC patient-derived cells[11,12], because β-CD can form an inclusion complex which cholesterol[9,13]. Furthermore, the administration of HP-β-CD reduces the cholesterol content in various organs, leading to a remarkable prolongation of the life-span of NPC1-deficient mice[14,15]. Nowadays, the clinical investigation on the therapeutic effect of HP-β-CD against NPC disease patient is demonstrated[16]. However, to obtain a sufficient therapeutic effect, a high dose of HP-β-CD is typically required (approximately 4,000 mg/kg against mice)[14,15]. This is most likely because systemically administered β-CD has a short half-life in bloodstream owing to its rapid renal clearance[17,18], non-specific interaction or inclusion of cholesterols and proteins in the bloodstream, and low ability to cross the cellular membrane[19,20]. Additionally, when the concentration of β-CD is high, there is a concern that it may have toxic effects such as hemolysis, cytotoxicity, apoptosis induction, and tissue injury[21–24]. Therefore, the therapeutic efficacy of HP-β-CD is limited due to its severe toxic effects.

To address these drawbacks, we focused on polyrotaxanes (PRXs) that consist of β-CDs threaded along a polymer chain capped with terminal bulky molecules (Fig. 1A)[25–27]. Especially, we have developed biocleavable polyrotaxanes bearing terminal disulfide linkages[28–31], because disulfide linkage is known to cleave intracellular environments through the reaction with L-glutathione (GSH)[32]. We have previously demonstrated α-CD-based biocleavable PRX as a delivery carrier for nucleic acids and proteins, and the PRX bearing terminal disulfide linkages exerts intracellular degradation via the reaction with intracellular GSH[28–31]. Herein, biocleavable PRXs

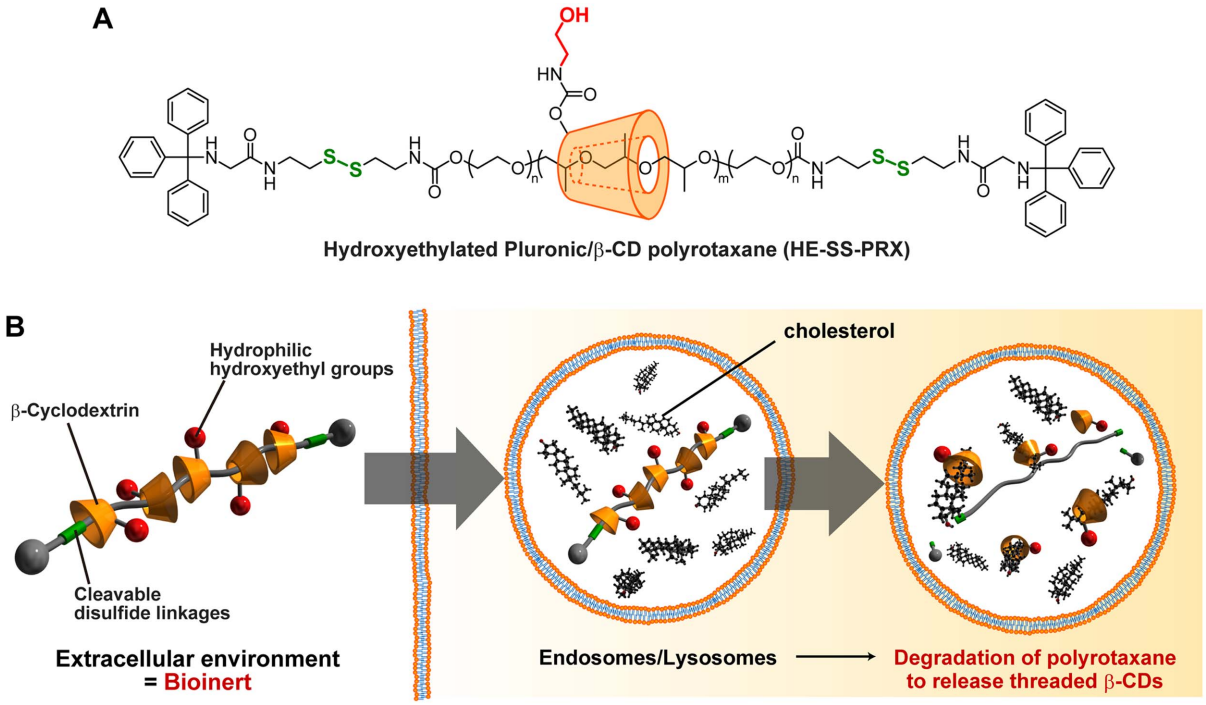

Figure 1 | Biocleavable polyrotaxanes (PRXs) as therapeutics for NPC disease. (A) Chemical structure of biocleavable PRXs bearing terminal disulfide linkages (HE-SS-PRX). (B) Schematic illustration of the intracellular dissociation of the PRXs and the subsequent lysosomal release of threaded β-CDs to improve cholesterol accumulation in NPC disease-derived cells.

have tremendous advantages that allow them to overcome all of the problems of β-CDs in NPC disease therapy: (1) masking of the toxic effect of β-CD derivatives, as the hydrophobic cavity of β-CD is occupied by a polymer chain to avoid non-specific inclusions; (2) retardation of renal clearance, thus prolonging blood half-life, because of its high molecular weight (typically 20,000 to 100,000, depending on the number of threaded CDs) in comparison with β-CD derivatives (approximately 1,000 to 1,500), (3) preferential accumulation in endosomes/lysosomes through endocytosis; and (4) the ability to release threaded β-CDs via cleaving the terminal linker of PRXs under intracellular environments to achieve therapeutic effect (Fig. 1B). Recently, β-CD-threaded polyrotaxanes have been reported for the removal of cholesterol accumulated in NPC2-deficient cells[33,34]. In those reports, there is no marked difference in the cholesterol removal efficiency between their PRXs and β-CD, probably due to the lack of cleavable linkers in PRX. Therefore, biocleavable PRXs are thought to show much effective cholesterol removal ability through the lysosomal release of threaded β-CDs.

In this study, we have designed β-CD-threaded biocleavable PRXs and investigated their toxicity and cholesterol reduction effect against NPC disease patient-derived cells in comparison with β-CD derivatives. Furthermore, the mechanism of action of biocleavable PRX and β-CD derivatives such as gene expression and intracellular distribution analysis were demonstrated in comparison with β-CD derivatives to better understand the feasibility of biocleavable PRX as therapeutics for NPC disease.

Results

Synthesis of biocleavable polyrotaxanes. To validate the concept of NPC disease therapy by β-CD-threaded PRXs, we have synthesized biocleavable hydroxyethylated PRXs composed of Pluronic P123 ($M_{n,PPG}$: 4,150, $M_{n,PEG}$: 1,100 × 2), β-CDs, and terminal disulfide linkages (HE-SS-PRX) (Supplementary Information)[28–31,35,36]. Hydroxyethyl (HE) groups were introduced on the β-CD moieties to give water-solubility to the PRXs[36]. The numbers of threaded β-CDs and modified HE groups on the HE-SS-PRX were determined to be 12.9 and 52, respectively. As a control, non-cleavable PRX without terminal disulfide linkages (HE-PRX) was synthesized[28–31], in which the number of threaded β-CDs and modified HE groups were determined to be 11.3 and 66, respectively (Supplementary Information).

Hemolytic activity and cytotoxicity of PRXs and β-CD derivatives. To verify whether the PRX structure can mask the toxic effects of β-CD, hemolytic activity against erythrocytes and cytotoxicity against NPC1 protein-deficient NPC disease patient-derived fibroblasts (NPC1 cells) were demonstrated in comparison with HP-β-CD and heptakis(2,6-di-O-methyl)-β-cyclodextrin (DM-β-CD), which has the highest binding ability to cholesterol (Fig. 2)[21]. DM-β-CD and HP-β-CD induced hemolysis of erythrocytes and cytotoxicity against NPC1 cells, which is consistent with a previous report[21–23]. On the contrary, the cleavable HE-SS-PRX and the non-cleavable HE-PRX showed negligible hemolysis and cytotoxicity even at the β-CD concentration of 20 mM. The hemolytic activity of the cleavable HE-SS-PRX was only observed in the presence of 5 mM of L-glutathione (GSH), which is a sufficient concentration to cleave the disulfide linkages of HE-SS-PRX (Supplementary Fig. S3)[28–31]. This is due to the hemolytic activity of dethreaded β-CDs from HE-SS-PRX upon the addition of GSH. Eventually, the PRX structure can completely mask the hemolytic activity and cytotoxicity of β-CD, indicating the bioinert characteristics of the PRX.

Intracellular cholesterol reduction in NPC1 cells. Next, the change in lysosomal cholesterol content and the enlargement of endosomes/lysosomes in NPC1 cells were observed by confocal laser scanning microscopy (CLSM) after the treatment with each sample for 24 h (β-CD concentration: 0.1 mM) (Fig. 3A). The NPC1 cells showed significant accumulation of cholesterol (filipin staining) and the enlargement of acidic endosomes/lysosomes (LysoTracker staining) compared to normal human fibroblasts[6,7]. At this low concentration (β-CD: 0.1 mM), no significant change in NPC1 phenotype was observed for HP-β-CD. DM-β-CD reduced the cholesterol content and the number of the endosomes/lysosomes moderately, presumably

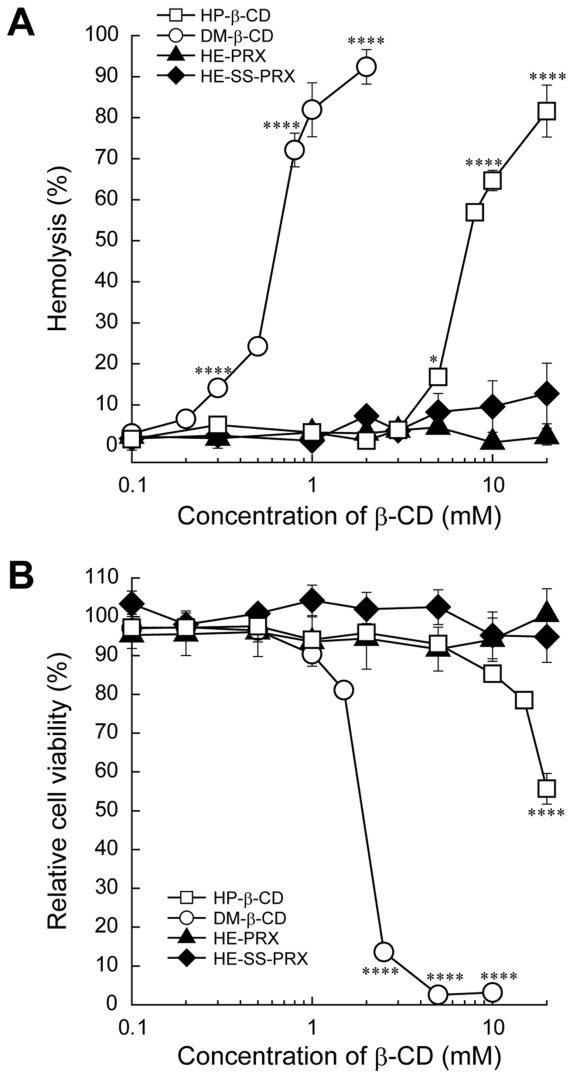

Figure 2 | Hemolytic activity and cytotoxicity of PRXs and β-CD derivatives. (A) Hemolysis of rat erythrocytes incubated with HP-β-CD, DM-β-CD, non-cleavable HE-PRX, and cleavable HE-SS-PRX at various β-CD concentrations for 2 h. Data are expressed as the mean ± S.D. (n = 3). (B) Viability of NPC1 cells incubated with HP-β-CD, DM-β-CD, non-cleavable HE-PRX, and cleavable HE-SS-PRX at various β-CD concentrations for 24 h. Data are expressed as the mean ± S.D. (n = 4) (*$p < 0.05$, **** $p < 0.001$).

owing to its strong ability to bind cholesterol[21]. The difference in the lysosomal cholesterol reduction ability between HP-β-CD and DM-β-CD is consistent with previous reports[11]. Although the non-cleavable HE-PRX-treated NPC1 cells showed no marked change in lysosomal cholesterol content and the enlargement of endosomes/lysosomes, the NPC1 cells treated with cleavable HE-SS-PRX demonstrated remarkable reductions in both the cholesterol content and the number of the endosomes/lysosomes to a level nearly comparable to that of normal cells.

Further investigation was demonstrated by quantifying the amount of total cholesterol in NPC1 cells after the treatment with PRXs or β-CD derivatives at various concentrations for 24 h (Fig. 3B). Being consistent with the previous reports, HP-β-CD reduced the total cholesterol content in NPC1 at high concentration. DM-β-CD also reduced the cholesterol content in NPC1 cells at lower concentration than HP-β-CD. Treatment with cleavable HE-SS-PRX reduced the cholesterol content in NPC1 cells even at the concentration below 0.1 mM, whereas non-cleavable HE-PRX treatment showed almost no effect even at the β-CD concentration of 10 mM. Accordingly, the half maximal effective concentration (EC_{50}) of HP-β-CD, DM-β-CD, and HE-SS-PRX were determined to be 2599 ± 548 μM, 234.3 ± 34.8 μM, and 24.2 ± 2.3 μM, respectively. The EC_{50} of HE-SS-PRX was 107-fold and 9.7-fold lower than HP-β-CD and DM-β-CD, respectively.

We also tested the cholesterol reduction ability of other bioclevable PRXs bearing acid-labile β-thiopropionate linkages or cyclic acetals (Supplementary Fig. S4)[37–39]. These types of bioclevable PRXs exert degradation by the hydrolysis under acidic endosomes and lysosomes. The EC_{50} values of acid-labile PRXs bearing β-thiopropionate linkages or cyclic acetals were determined to be 48.6 ± 6.5 μM, and 131.4 ± 59.9 μM, respectively, which are slightly higher than that of HE-SS-PRX. Therefore, it is considered that the reduction-cleavable disulfide linkages are the suitable linker to induce intracellular degradation of PRX to release threaded β-CDs.

The sustainability of the cholesterol reduction effect is of interest for determining the optimal dose frequency of therapeutics. Fig. 3C shows the time-course of total cholesterol content in NPC1 cells after 24 h incubation with the various treatment solutions, followed by incubation for the indicated time period without treatments. To adjust the total cholesterol content at 24 h, the β-CD concentration was varied among tested samples. After the removal of the samples from the medium, the cholesterol content gradually increased in a time-dependent manner. However, HE-SS-PRX showed the most sustained cholesterol reduction, and the cellular cholesterol content at 96 h incubation was significantly lower than that of cells treated with HP-β-CD and DM-β-CD.

Gene expression analysis of NPC1 cells treated with HE-SS-PRX and HP-β-CD. The HP-β-CD is known to preferentially excrete the cholesterol from the plasma membrane[40,41], which induces to recruit the cholesterol from the endoplasmic reticulum (ER) to the plasma membrane[42,43]. Sterol regulatory element-binding protein-2 (SREBP-2) is a transcription factor for cholesterol accretion and it plays central role to detect the concentration of cholesterol in ER[44]. When the ER cholesterol is recruited to the plasma membrane, the concentration of cholesterol in ER is temporarily reduced, which leads to SREBP-2 processing and upregulating the expression level of mRNAs related to cholesterol biosynthesis and uptake, such as 3-hydroxy-3-methylglutaryl-coenzyme A reductase (HMGCR), 3-hydroxy-3-methylglutaryl-coenzyme A synthase (HMGCS), and low-density lipoprotein receptor (LDLR)[44]. Therefore, to better understanding the mechanism of action of HE-SS-PRX, the ability to excrete cholesterol from the plasma membrane (Fig. 4A) and mRNA expression level of NPC1 cells (Fig. 4B) were evaluated in comparison with HP-β-CD. After the treatment of NPC1 cells in short time (1 h), the concentration of cholesterol in the medium was increased for HP-β-CD. On the contrary, negligible change in the concentration of cholesterol in the medium was observed for HE-SS-PRX, indicating that the PRX has no ability to excrete cholesterols from the plasma membrane. The mRNA expression level of SREBP-2, HMGCR, HMGCS, and LDLR in NPC1 cells were evaluated after treatment with HE-SS-PRX or HP-β-CD (Fig. 4B). After 24 h incubation with HP-β-CD, the level of these mRNAs was significantly upregulated, which is consistent with observations in NPC1-deficient neurons[12]. On the contrary, HE-SS-PRX was found to induce negligible upregulation of these mRNAs in NPC1 cells.

Cellular association and intracellular distribution analysis of HE-SS-PRX and HP-β-CD. To clarify why the cleavable HE-SS-PRX has a remarkably superior ability to reduce accumulated cholesterols compared to HP-β-CD, the cellular association level of HE-SS-PRX and HP-β-CD was investigated by flow cytometry using fluorescein isothiocyanate (FITC)-labeled HE-SS-PRX (FITC-HE-SS-PRX) and HP-β-CD (FITC-HP-β-CD) during 24 h of incubation (Fig. 5A). Although FITC-HE-SS-PRX showed a

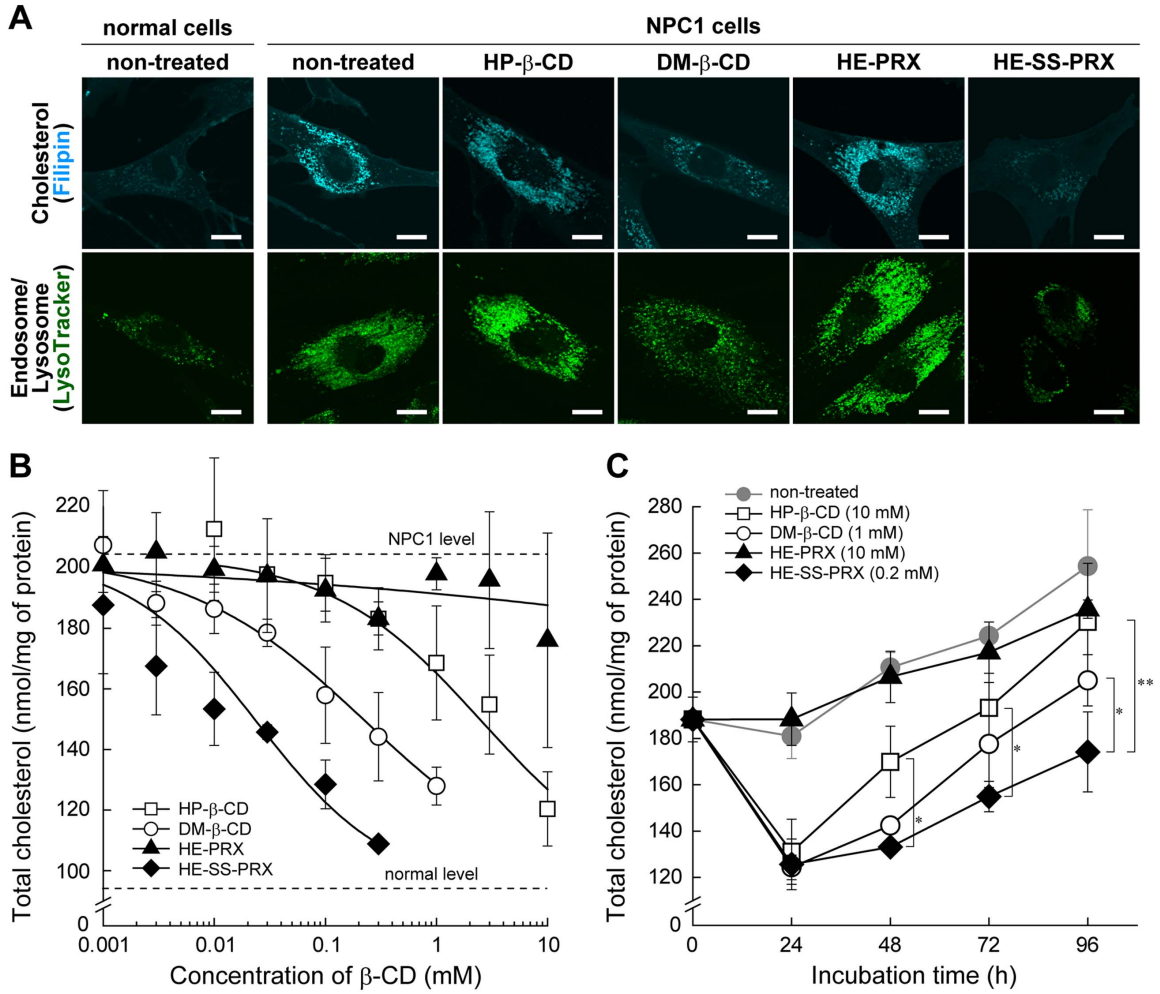

Figure 3 | Lysosomal cholesterol reduction ability of biocleavable HE-SS-PRX against NPC1 cells. (A) Filipin staining for unesterified cholesterol and LysoTracker staining for endosome/lysosome in normal and NPC1 cells (bar: 20 μm). The NPC1 cells were incubated with HP-β-CD, DM-β-CD, non-cleavable HE-PRX, and cleavable HE-SS-PRX at the β-CD concentration of 0.1 mM for 24 h. (B) The amount of intracellular total cholesterol in NPC1 cells incubated with HP-β-CD, DM-β-CD, non-cleavable HE-PRX, and cleavable HE-SS-PRX at various β-CD concentrations for 24 h. The dashed lines represent the amount of intracellular total cholesterol in non-treated normal and NPC1 cells. (C) Time-course of the amount of intracellular total cholesterol in NPC1 cells after incubation with HP-β-CD (β-CD: 10 mM), DM-β-CD (β-CD: 1 mM), non-cleavable HE-PRX (β-CD: 10 mM), and cleavable HE-SS-PRX (β-CD: 0.2 mM) for 24 h, followed by incubation without treatment for the indicated time periods. The closed circles represent the non-treated NPC1 cells. Data are expressed as the mean ± S.D. (n = 3) (*$p < 0.05$, ** $p < 0.01$).

slightly higher cellular association level than FITC-HP-β-CD, it is inconsistent with the 107-fold difference in EC_{50} values between HE-SS-PRX and HP-β-CD. However, the CLSM observation revealed that most of the FITC-HE-SS-PRX appeared within the intracellular region of NPC1 cells, and the intracellular uptake level of FITC-HE-SS-PRX increased with time. In sharp contrast, FITC-HP-β-CD was found to accumulated at the cell periphery during the exposure time period, probably due to its strong interaction with the plasma membranes (Fig. 5B)[13,19]. To clarify the details of the intracellular localization of HE-SS-PRX and HP-β-CD, early endosomes, late endosomes, and lysosomes were stained with early endosome antigen 1 (EEA1), CD63, and lysosomal-associated membrane protein 1 (LAMP1) antibodies[45], and colocalization percentage of HE-SS-PRX and HP-β-CD to these compartments was determined from the resulting images (Fig. 5C,D). Although the cholesterols accumulation of NPC1 cells is known to occur in late endosomes or lysosomes, most of the FITC-SS-PRX was found to be localized in late endosomes or lysosomes. On the contrary, colocalization of FITC-HP-β-CD to these compartments was negligible.

The result described above also suggests that if the amount of β-CD transported into late endosomes and lysosomes is increased, the cholesterol reduction ability can be further facilitated. We have previously demonstrated that tertiary amino group-modified PRX has superior intracellular uptake via endocytosis in comparison to conventional linear polymers[46]. Therefore, we investigated the cholesterol reduction in NPC1 cells that was treated with *N*,*N*-dimethylaminoethyl groups-modified PRXs (DMAE-SS-PRX; number of threaded β-CDs: 12.9, number of DMAE groups: 65.3) (Fig. 6A). The CLSM observation revealed that the cellular uptake level of cationic DMAE-SS-PRX was remarkably higher than nonionic HE-SS-PRX (Fig. 6B). Eventually, DMAE-SS-PRX showed approximately 20-fold higher preferential cellular internalization than HE-SS-PRX as determined by flow cytometry (Fig. 6C). Treatment of NPC1 cells with DMAE-SS-PRX resulted in greater cholesterol reduction ability in comparison with HE-SS-PRX treatment (Fig. 6D). The EC_{50} value of DMAE-SS-PRX is determined to be 2.8 ± 0.4 μM, which is approximately 9.3-fold and 928-fold lower than HE-SS-PRX and HP-β-CD, respectively.

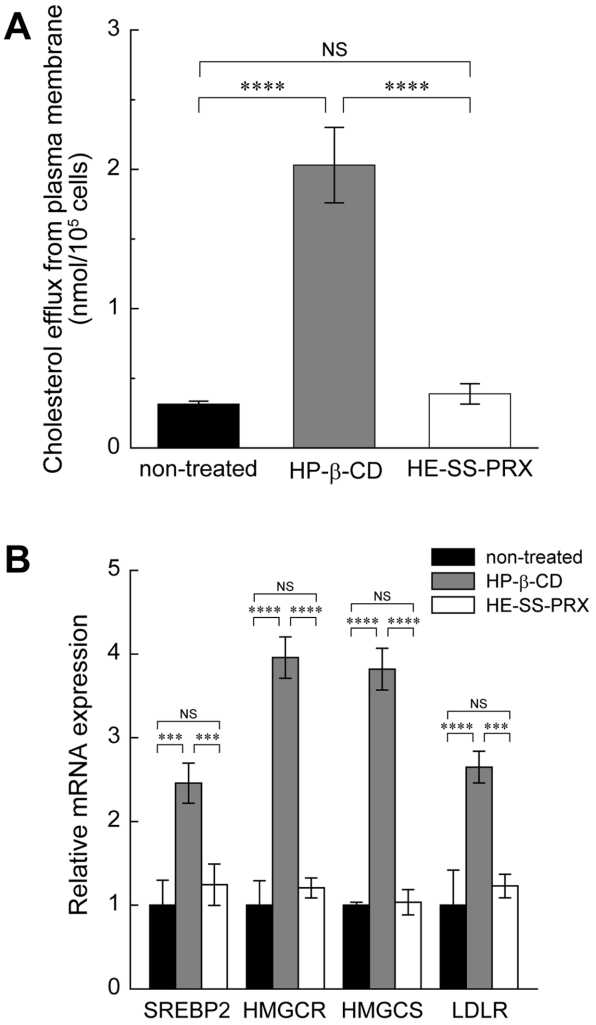

Figure 4 | Cholesterol efflux from the plasma membrane and gene expression analysis for HE-SS-PRX and HP-β-CD treatment. (A) The amount of cholesterol efflux from the plasma membrane of NPC1 cells after 1 h incubation with HP-β-CD and HE-SS-PRX at 37°C. The concentration of β-CD is 10 mM. (B) Relative mRNA expression levels of SREBP-2, HMGCR, HMGCS, and LDLR in NPC1 cells after incubation with HP-β-CD (β-CD: 10 mM) or HE-SS-PRX (β-CD: 0.2 mM) for 24 h at 37°C. Data are normalized to the expression level of β-actin. Data are expressed as the mean ± S.D. (n = 3) (***$p < 0.005$, ****$p < 0.001$, NS indicates not significant).

Discussion

In this study, we have demonstrated the therapeutic potential of β-CD-threaded biocleavable PRXs for NPC disease. Although the β-CD derivatives are expected as a promising therapeutics for NPC disease therapy, they have a drawback of toxic concern, especially at high concentration[21–24]. We found that the PRX structure is beneficial to mask the toxic effect of β-CD (Fig. 2). Since the hydrophobic cavity of β-CD is occupied with a polymer chain in PRX, it shows low interaction with the plasma membrane, resulting in negligible excretion of cholesterols from the plasma membrane (Fig. 4A, 5B). The cholesterol removal from the plasma membrane by CD disrupts the membrane integrity and fluidity to induce hemolysis and apoptosis[21,23]. Therefore, the unique supramolecular structure of PRX is essential to overcome the toxic effect of β-CD derivatives.

The biocleavable PRX has also appealing property to release threaded β-CDs under intracellular environments. The lysosomal cholesterol reduction ability is significantly enhanced by the biocleavable PRX compared to β-CD derivatives (Fig. 3A,B). Also, the comparison study between biocleavable and non-cleavable PRXs give us an important insight that the intracellular release of threaded β-CDs from PRX is essential to achieve the reduction of lysosomal cholesterol accumulation. From the result of CLSM observation, the release of threaded β-CDs from PRX is thought to occur in these compartments. The lysosomal release of threaded β-CDs from PRX increases the local concentration of β-CDs to exert higher lysosomal cholesterol reduction compared to β-CD derivatives. It is believed that intracellular GSH is stored in cytoplasm, and the endosomal and lysosomal concentration of GSH is lower than cytoplasm. Since the pH value of late endosomes and lysosomes is lowered to 4.5 to 6.0[47], we considered that the acid-labile PRX is more effective to release β-CDs under late endosomes and lysosomes than reduction-cleavable HE-SS-PRX. However, the lysosomal cholesterol reduction ability of the acid-labile PRX bearing β-thiopropionate linkages or cyclic acetals is lower than HE-SS-PRX. Therefore, it is suggested that the HE-SS-PRX is degraded in lysosomes by the enzymatic disulfide cleavage such as gamma-interferon-inducible lysosomal thiol reductase (GILT)[48]. Although the detailed degradation mechanism of HE-SS-PRX in late endosomes and lysosomes is not fully clarified, it should be noted that the lysosomal β-CD release from PRX plays pivotal role in effective cholesterol reduction in NPC1 cells.

Additionally, the bioinert character of HE-SS-PRX allowed endocytosis to transport into the late endosomes and lysosomes (Fig. 5C,D). On the contrary, since most of the β-CD derivatives are localized at the plasma membrane owing to their strong interaction, it is difficult to reach intracellular environment. It is therefore conceivable that the significant difference in EC_{50} values between HE-SS-PRX and HP-β-CD might be due to the difference in localization to late endosomes and lysosomes. Additionally, we found that the enhancement of intracellular uptake amount of PRX by the introduction of cationic DMAE groups resulted in further lowered ED_{50} value (Fig. 6). Although DMAE-SS-PRX is not suitable for practical use owing to its polycation toxicity, both the amount of cellular internalization and the lysosomal localization of PRX have been proved to be essential for reducing accumulated cholesterols.

Rosenbaum et al. have demonstrated the sustainability of cholesterol reduction ability of HP-β-CD derivatives in NPC1 and NPC2 cells[11]. After the removal of HP-β-CD from medium, the intracellular concentration of cholesterol is gradually increased. Our result of HP-β-CD is consistent with their report. Interestingly, we found that the cholesterol reduction by biocleavable PRX is more sustainable than HP-β-CD. HP-β-CD is known to facilitate the transfer of lysosomal cholesterol to ER to suppress the SREBP-2 processing[49]. However, we found that high concentration of HP-β-CD (10 mM) induced the upregulation of the SREBP-2 mRNA level, probably due to the depletion of cholesterol from the plasma membrane. This leads to activating the inherited cholesterol biosynthesis (HMGCR and HMGCS) and uptake (LDLR) machinery (Fig. 4B); therefore, HP-β-CD treatment increases intracellular cholesterol level again through the uptake of LDL-derived cholesterols. By contrast, HE-SS-PRX does not activate cholesterol biosynthesis and uptake, resulting in sustainable cholesterol reduction compared to HP-β-CD (Fig. 3C).

In summary, this study demonstrates the feasibility of biocleavable polyrotaxanes as therapeutics for NPC1 disease. HE-SS-PRX is found to avoid non-specific interaction with the plasma membrane to achieve preferential lysosomal accumulation, and the biocleavable nature of HE-SS-PRXs increases the local concentration of β-CD in late endosomes/lysosomes, leading to a remarkable enhancement in the effect of lysosomal cholesterol reduction in NPC1 cells. Accordingly, the cleavable PRXs are thought to be noninvasive and effective therapeutics for the NPC diseases. To elucidate the concept of biocleavable PRXs as therapeutics for NPC disease, further studies along with in vivo pharmacological effect, body disposition, and safety are required. Since the PRXs have higher molecular weight than β-CD derivatives, they are expected to avoid renal clearance,

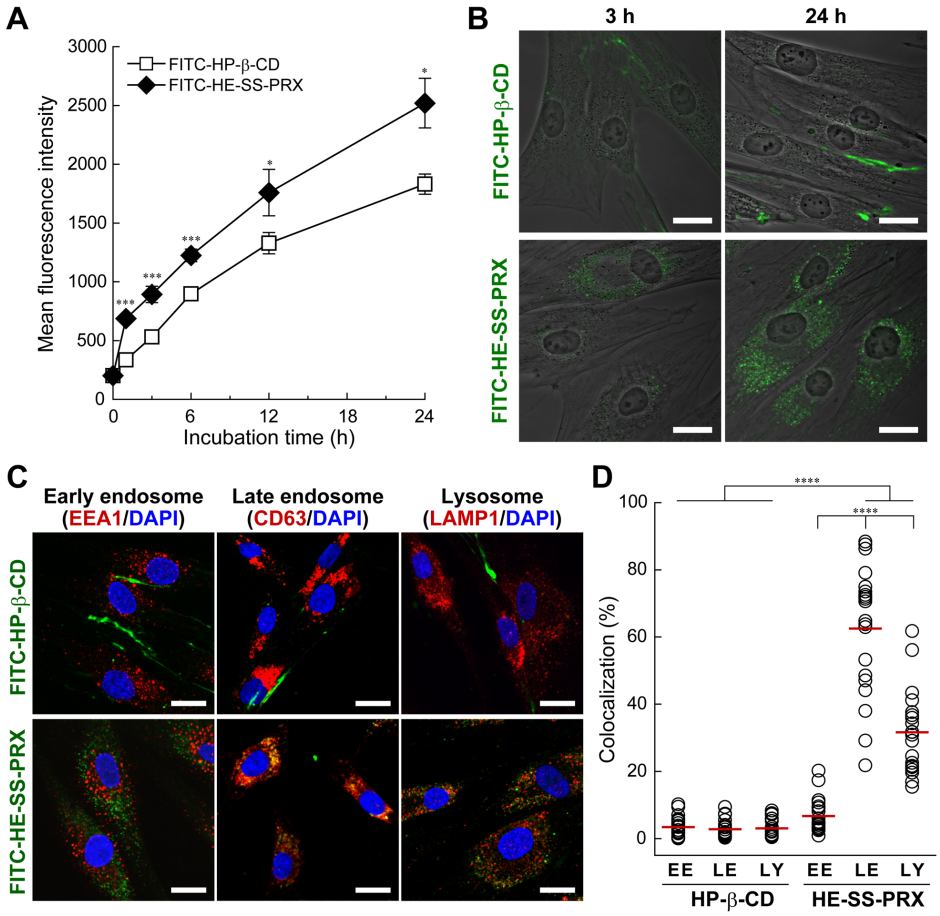

Figure 5 | Cellular association and intracellular distribution of fluorescently-labeled HE-SS-PRX and HP-β-CD. (A) Time-course of the mean fluorescence intensity of NPC1 cells incubated with FITC-HP-β-CD (β-CD: 0.5 mM) and FITC-HE-SS-PRX (β-CD: 0.5 mM). (B) CLSM images of NPC1 cells incubated with FITC-HP-β-CD (green, β-CD: 0.5 mM) and FITC-HE-SS-PRX (green, β-CD: 0.5 mM) for 3 h and 24 h (bar: 20 μm). (C) Intracellular distribution analysis of FITC-HP-β-CD (green, β-CD: 0.5 mM) and FITC-HE-SS-PRX (green, β-CD: 0.5 mM) in NPC1 cells after incubation for 24 h (bar: 20 μm). The early endosomes, late endosomes, and lysosomes are stained with EEA1, CD63, and LAMP1 antibodies, respectively (red). The nuclei are stained with DAPI (blue). (D) Colocalization percentage of FITC-HP-β-CD and FITC-HE-SS-PRX to early endosomes (EE), late endosomes (LE), and lysosomes (LY) after 24 h as determined from CLSM images. The bars represent the means of 20 cells (*$p < 0.05$, ***$p < 0.005$, ****$p < 0.001$).

resulting in a prolonged blood circulation time. This prolonged blood circulation might contribute to increasing the accumulation level of β-CDs in various tissues, leading to effectively reducing the tissue cholesterol level in comparison to β-CD derivatives. In addition, although the PRXs were revealed to show negligible toxicity under in vitro condition, we have to provide enough evidence of PRX safety under in vivo condition. These investigations are currently underway in our laboratory.

Methods

Synthesis of biocleavable polyrotaxanes. Pluronic P123, a triblock copolymer of poly(ethylene glycol) (PEG)-*b*-poly(propylene glycol) (PPG)-*b*-PEG, was obtained from Sigma-Aldrich (Milwaukee, WI, USA). The number of monomer repeating units in PEG and PPG segments were determined to be 25.2 × 2 ($M_{n,PEG}$: 1,100 × 2) and 71.5 ($M_{n,PPG}$: 4,150), respectively, by ^{1}H nuclear magnetic resonance (NMR) spectroscopy. The synthesis of biocleavable HE-SS-PRX and non-cleavable HE-PRX were described in Supplementary Information.

Hemolysis assay. The rat erythrocyte suspensions (2 × 10^8 cells/mL, 100 μL) (Kohjin Bio, Saitama, Japan) were incubated with the treatment solutions (100 μL) for 2 h at 37°C. Then, the erythrocytes were separated by centrifugation (2,000 rpm for 5 min) and the supernatant (100 μL) was collected. The amount of released hemoglobin was determined by reading the absorbance at 540 nm on a Multiskan FC plate reader (Thermo Fisher Scientific, Waltham, MA, USA). To determine the absorbance of 100% hemolysis, erythrocytes were lysed with 0.1% Triton X-100 (Sigma-Aldrich). The hemolytic activities were calculated relative to the 0.1% Triton X-100-treated samples.

Cell culture. Human dermal fibroblasts derived from a Niemann-Pick type C disease patient (NPC1) (GM03123) and a normal human dermal fibroblast (GM05659) were obtained from the Coriell Institute for Medical Research (Camden, NJ, USA) and grown in Dulbecco's modified eagle medium (DMEM) (Gibco BRL, Grand Island, NY, USA) containing 10% fetal bovine serum (FBS) (Gibco), 100 units/mL penicillin, and 100 μg/mL streptomycin (Gibco) in a humidified 5% CO_2 atmosphere at 37°C.

Cytotoxicity assay. NPC1 cells were seeded on a 96-well plate (BD Falcon, Franklin Lakes, NJ, USA) at a density of 1 × 10^4 cells/well and incubated overnight. After the medium was exchanged for fresh DMEM (90 μL), the sample solutions (10 μL) were applied to each well. After incubation for a further 24 h, Cell Counting Kit-8 reagent (Dojindo Laboratories, Kumamoto, Japan) (10 μL) was added to each well. After further incubation for 1 h at 37°C, the absorbance at 450 nm was measured on a Multiskan FC plate reader. The cellular viability was calculated relative to the non-treated cells.

Filipin staining for cholesterol. NPC1 or normal cells were seeded on 35-mm glass-bottomed dishes (Greiner Bio-one, Frickenhausen, Germany) at a density of 1 × 10^4 cells/dish and incubated overnight. After the medium was exchanged with fresh DMEM (900 μL), the treatment solutions (100 μL) were applied to the dish. After incubation for 24 h, the cells were washed twice with PBS and fixed with 4% paraformaldehyde for 15 min at room temperature. The cells were stained with filipin (PolySciences, Warrington, PA, USA) (50 μg/mL) for 45 min at room temperature. The confocal laser scanning microscopic (CLSM) observations were performed on a FluoView FV10i (Olympus, Tokyo, Japan) equipped with a 60× water-immersion objective lens (N/A 1.2) and a diode laser.

LysoTracker staining for acidic endosome/lysosome. NPC1 or normal cells were seeded on 35-mm glass-bottomed dishes at a density of 1 × 10^4 cells/dish and

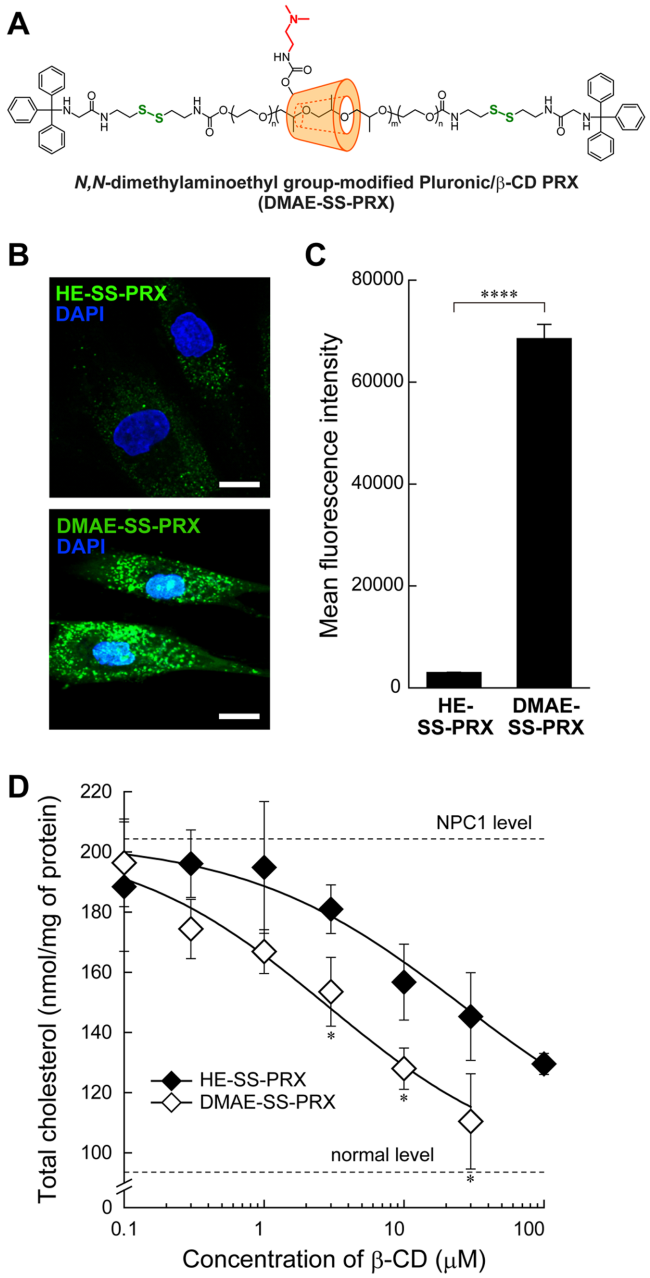

Figure 6 | Intracellular uptake and cholesterol reduction in NPC1 cells treated with cationic DMAE-SS-PRX. (A) Chemical structure of *N,N*-dimithylaminoethyl group-modified cationic PRXs bearing terminal disulfide linkages (DMAE-SS-PRX). (B) CLSM images of NPC1 cells incubated with nonionic FITC-HE-SS-PRX (green, β-CD: 0.25 mM) and cationic FITC-DMAE-SS-PRX (green, β-CD: 0.25 mM) for 24 h (bars: 20 μm). The nuclei are stained with DAPI (blue). (C) Mean fluorescence intensity of NPC1 cells incubated with nonionic FITC-HE-SS-PRX (β-CD: 0.25 mM) and cationic FITC-DMAE-SS-PRX (β-CD: 0.25 mM) for 24 h. (D) The amount of intracellular total cholesterol in NPC1 cells incubated with nonionic HE-SS-PRX or cationic DMAE-SS-PRX at various β-CD concentrations for 24 h. The dashed lines represent the amount of intracellular total cholesterol in non-treated normal and NPC1 cells. Data are expressed as the mean ± S.D. (n = 3) (*$p < 0.05$, ****$p < 0.001$).

incubated overnight. After the medium was exchanged with fresh DMEM (900 μL), the sample solutions (100 μL) were applied to the dish. After incubation for 24 h, the cells were washed twice with PBS and stained with LysoTracker Green DND-26 (Molecular Probes) (200 nM) for 10 min at 37°C. The CLSM observations were performed on a FluoView FV10i.

Cellular total cholesterol content. NPC1 or normal cells were seeded on a 24-well plate (BD Falcon) at a density of 2.5×10^4 cells/well and incubated overnight. After the medium was exchanged with fresh medium (270 μL), the treatment solutions (30 μL) were applied to each well. After incubation for 24 h, the cells were washed twice with PBS. Then, the cells were harvested and lysed with cell lysis buffer (50 mM phosphate buffer, 500 mM NaCl, 25 mM cholic acid, and 0.5% Triron X-100). The cellular total cholesterol was determined by Amplex Red Cholesterol Assay Kit (Molecular Probes) according to the manufacturer's instructions. After incubation for 30 min at 37°C, the fluorescence intensities were measured on an ARVO MX multilabel counter (Perkin Elmer, Wellesley, MA, USA) equipped with a filter set for excitation and emission at 560 ± 10 nm and 590 ± 10 nm, respectively. The total cholesterol content was calculated with a cholesterol standard curve. Cellular protein content was determined with a Micro BCA Protein Assay Kit (Thermo Fisher Scientific). Cellular cholesterol content was normalized to protein content.

Cholesterol efflux from the plasma membrane[19,24]. NPC1 or normal cells were seeded on a 24-well plate at a density of 1×10^5 cells/well and incubated overnight. After the medium was exchanged with PBS (270 μL), the treatment solutions (30 μL) were applied to each well. After incubation for 1 h at 37°C, the supernatant was collected. The concentration of cholesterol in the supernatant was determined by Amplex Red Cholesterol Assay Kit, as described above.

Quantitative gene expression analysis by real-time RT-PCR. NPC1 cells were seeded on a 24-well plate at a density of 2.5×10^4 cells/well and incubated overnight. After the medium was exchanged with fresh DMEM (270 μL), the treatment solutions (30 μL) were applied to each well. After incubation for 24 h, total RNA was isolated with a QIAshredder and RNeasy Mini Kit (Qiagen, Valencia, CA) according to the manufacturer's instructions. Then, cDNA was synthesized from 5 μg of the total RNA using iScript Advanced cDNA Synthesis Kit (Bio-Rad, Hercules CA). The real-time RT-PCR was performed on a CFX Connect real time PCR detection system (Bio-Rad). The final reaction mixture contained 2 μL of cDNA, 500 nM of each primer, 10 μL SsoAdvanced SYBR Green Supermix (Bio-Rad), and RNase/DNase-free water to complete the reaction mixture volume of 20 μL. Thermal cycling was performed for 40 cycles at 95°C for 10 s and at 60°C for 30 s. The sequences of the primer sets for amplification were summarized in Supplementary Table S1[50]. Gene expression levels were calculated using the ΔΔCt method, and the data were normalized with the expression level of β-actin.

Cellular association analysis for FITC-labeled HP-β-CD and HE-SS-PRX by flow cytometry. NPC1 cells were seeded on a 24-well plate at a density of 2.5×10^4 cells/cm² and incubated overnight. After the medium was exchanged with fresh medium (270 μL), the treatment solutions (30 μL) were applied to each well. After incubation for the indicated time periods, the cells were washed twice with PBS and harvested by trypsin-EDTA treatment. Then, the cells were collected by centrifugation (1000 rpm, 4°C, 5 min), and fixed with 2% paraformaldehyde for 20 min at room temperature. The cells were washed three times with PBS containing 0.1% bovine serum albumin (BSA) (Sigma-Aldrich) and passed through a 35 μm cell strainer (BD Falcon). The fluorescence intensity of the cells was determined by flow cytometry (FACSCanto II, BD Biosciences). The FITC-labeled samples were excited using 20 mW solid-state laser (488 nm) and detected with a 515–545 nm bandpass filter. A total of 10,000 cells were acquired for each sample and the mean fluorescence intensity of cell population was analyzed by DIVA software (BD Biosciences).

Intracellular distribution analysis for FITC-labeled HP-β-CD and HE-SS-PRX by CLSM. NPC1 or normal cells were seeded on 35-mm glass-bottomed dishes at a density of 1×10^4 cells/dish and incubated overnight. After the medium was exchanged with fresh DMEM (900 μL), the treatment solutions (100 μL) were applied to the dish. After the cells were incubated with FITC-labeled HP-β-CD and HE-SS-PRX for 24 h, the cells were washed twice with PBS, fixed with 4% paraformaldehyde for 15 min at room temperature, and permeabilized with 0.1% Triton X-100 for 10 min at room temperature. Then, the cells were treated with mouse anti-human early endosome antigen 1 (EEA1) antibody (clone: 14/EEA1) (BD Biosciences) (1 : 100 dilution), mouse anti-human CD63 antibody (clone: H5C6) (BioLegend, San Diego, CA, USA) (1 : 200 dilution), or mouse anti-human lysosomal-associated membrane protein 1 (LAMP1) antibody (clone: H4A3) (Santa Cruz Biotechnology, Santa Cruz, CA, USA) (1 : 50 dilution) for 1 h at room temperature. After three washes with PBS, the cells were stained with Alexa Fluor 647-labeled goat anti-mouse IgG (Abcam, Cambridge, MA, USA) (1 : 1000 dilution) for 30 min at room temperature. Then, the cells were stained with 4′,6-diamidino-2-phenylindole (DAPI) (Dojindo Laboratories) (1 μg/mL) for 10 min at room temperature. The CLSM observations were performed on a FluoView FV10i and the colocalization percentage was analyzed using FluoView Viewer (Olympus).

Statistical analysis. The data are presented as the mean ± standard deviation (S.D.). Differences between the means of individual groups were assessed by one-way analysis of variance (ANOVA) followed by Tukey's multiple comparison test. A *p*-value of less than 0.05 was considered as statistically significant. The statistical analysis was performed using OriginPro 8 (OriginLab, MA, USA).

1. Futerman, A. H. & van Meer G. The cell biology of lysosomal storage disorders. *Nat. Rev. Mol. Cell Biol.* **5**, 554–565 (2004).

2. Chang, T.-Y. *et al.* Niemann-Pick type C disease and intracellular cholesterol trafficking. *J. Biol. Chem.* **280**, 20917–20920 (2005).
3. Vanier, M. T. & Millat, G. Niemann-Pick disease type C. *Clin. Genet.* **64**, 269–281 (2003).
4. Carstea, E. D. *et al.* Niemann-Pick C1 disease gene: homology to mediators of cholesterol homeostasis. *Science* **277**, 228–231 (1997).
5. Griffin, L. D., Gong, W., Verot, L. & Mellon, S. H. Niemann–Pick type C disease involves disrupted neurosteroidogenesis and responds to allopregnanolone. *Nat. Med.* **10**, 704–711 (2004).
6. Lloyd-Evans, E. *et al.* Niemann-Pick disease type C1 is a sphingosine storage disease that causes deregulation of lysosomal calcium. *Nat. Med.* **14**, 1247–1255 (2008).
7. Xu, M. *et al.* δ-Tocopherol reduces lipid accumulation in Niemann-Pick type C1 and Wolman cholesterol storage disorders. *J. Biol. Chem.* **287**, 39349–39360 (2012).
8. Davis, M. E. & Brewster, M. E. Cyclodextrin-based pharmaceutics: past, present and future. *Nat. Rev. Drug Discov.* **3**, 1023–1035 (2004).
9. Irie, T. & Uekama, K. Cyclodextrins in peptide and protein delivery. *Adv. Drug Deliv. Rev.* **36**, 101–123 (1999).
10. Liu, B. Therapeutic potential of cyclodextrins in the treatment of Niemann-Pick type C disease. *Clin. Lipidol.* **7**, 289–301 (2012).
11. Rosenbaum, A. I., Zhang, G., Warren, J. D. & Maxfield, F. R. Endocytosis of beta-cyclodextrins is responsible for cholesterol reduction in Niemann-Pick type C mutant cells. *Proc. Natl. Acad. Sci. USA* **107**, 5477–5482 (2010).
12. Peake, K. B. & Vance, J. E. Normalization of cholesterol homeostasis by 2-hydroxypropyl-β-cyclodextrin in neurons and glia from Niemann-Pick C1 (NPC1)-deficient mice. *J. Biol. Chem.* **287**, 9290–9298 (2012).
13. Yancey, P. G. *et al.* Cellular cholesterol efflux mediated by cyclodextrins. Demonstration of kinetic pools and mechanism of efflux. *J. Biol. Chem.* **27**, 16026–16034 (1996).
14. Liu, B. *et al.* Reversal of defective lysosomal transport in NPC disease ameliorates liver dysfunction and neurodegeneration in the npc1$^{-/-}$ mouse. *Proc. Natl. Acad. Sci. USA* **106**, 2377–2382 (2009).
15. Davidson, C. D. *et al.* Chronic cyclodextrin treatment of murine Niemann-Pick C disease ameliorates neuronal cholesterol and glycosphingolipid storage and disease progression. *PLoS One* **4**, e6951 (2009).
16. Matsuo, M. *et al.* Effects of cyclodextrin in two patients with Niemann-Pick type C disease. *Mol. Genet. Metab.* **108**, 76–81 (2013).
17. Frijlink, H. W. *et al.* The pharmacokinetics of β-cyclodextrin and hydroxypropyl-β-cyclodextrin in the rat. *Pharm. Res.* **7**, 1248–1252 (1990).
18. Gould, S. & Scott, R. C. 2-Hydroxypropyl-β-cyclodextrin (HP-β-CD): a toxicology review. *Food. Chem. Toxicol.* **43**, 1451–1459 (2005).
19. Onodera, R. *et al.* Involvement of cholesterol depletion from lipid rafts in apoptosis induced by methyl-β-cyclodextrin. *Int. J. Pharm.* **452**, 116–123 (2013).
20. Kilsdonk, E. P. *et al.* Cellular cholesterol efflux mediated by cyclodextrins. *J. Biol. Chem.* **270**, 17250–17256 (1995).
21. Irie, T. & Uekama, K. Pharmaceutical applications of cyclodextrins. III. toxicological issues and safety evaluation. *J. Pharm. Sci.* **86**, 147–162 (1997).
22. Leroy-Lechat, F., Wouessidjewe, D., Andreux, J.-P., Puisieux, F. & Duchêne, D. Evaluation of the cytotoxicity of cyclodextrins and hydroxypropylated derivatives. *Int. J. Pharm.* **101**, 97–103 (1994).
23. Motoyama, K. *et al.* Involvement of PI3K-Akt-Bad pathway in apoptosis induced by 2,6-di-*O*-methyl-β-cyclodextrin, not 2,6-di-*O*-methyl-α-cyclodextrin, through cholesterol depletion from lipid rafts on plasma membranes in cells. *Eur. J. Pharm. Sci.* **38**, 249–261 (2009).
24. Onodera, R., Motoyama, K., Okamatsu, A., Higashi, T. & Arima, H. Potential use of folate-appended methyl-β-cyclodextrin as an anticancer agent. *Sci. Rep.* **3**, 1104; DOI:10.1038/srep01104 (2013).
25. Harada, A., Li, J. & Kamachi, M. The molecular necklace: a rotaxane containing many threaded α-cyclodextrins. *Nature* **356**, 325–327 (1992).
26. Wenz, G., Han, B. H. & Müller, A. Cyclodextrin rotaxanes and polyrotaxanes. *Chem. Rev.* **106**, 782–817 (2006).
27. Li, J. & Loh, X. J. Cyclodextrin-based supramolecular architectures: syntheses, structures, and applications for drug and gene delivery. *Adv. Drug Deliv. Rev.* **60**, 1000–1017 (2008).
28. Ooya, T. *et al.* Biocleavable polyrotaxane-plasmid DNA polyplex for enhanced gene delivery. *J. Am. Chem. Soc.* **128**, 3852–3853 (2006).
29. Yamashita, A. *et al.* Synthesis of a biocleavable polyrotaxane-plasmid DNA (pDNA) polyplex and its use for the rapid nonviral delivery of pDNA to cell nuclei. *Nat. Protoc.* **1**, 2861–2869 (2006).
30. Tamura, A. *et al.* Molecular logistics using cytocleavable polyrotaxanes for the reactivation of enzymes delivered in living cells. *Sci. Rep.* **3**, 2252; DOI:10.1038/srep02252 (2013).
31. Tamura, A. & Yui, N. Cellular internalization and gene silencing of siRNA polyplexes by cytocleavable cationic polyrotaxanes with tailored rigid backbones. *Biomaterials* **34**, 2480–2491 (2013).
32. Meng, F., Hennink, W. E. & Zhong, Z. Reduction-sensitive polymers and bioconjugates for biomedical applications. *Biomaterials* **30**, 2180–2198 (2009).
33. Collins, C. J. *et al.* Synthesis, characterization, and evaluation of pluronic-based β-cyclodextrin polyrotaxanes for mobilization of accumulated cholesterol from Niemann-Pick type C fibroblasts. *Biochemistry* **52**, 3242–3253 (2013).
34. Mondjinou, Y. A. *et al.* Synthesis of 2-hydroxypropyl-β-cyclodextrin/pluronic-based polyrotaxanes via heterogeneous reaction as potential Niemann-Pick type C therapeutics. *Biomacromolecules* **14**, 4189–4197 (2013).
35. Fujita, H. Ooya, T. & Yui, N. Thermally induced localization of cyclodextrins in a polyrotaxane consisting of β-cyclodextrins and poly(ethylene glycol)-poly(propylene glycol) triblock copolymer. *Macromolecules* **32**, 2534–2541 (1999).
36. Yui, N. *et al.* Inhibitory effect of supramolecular polyrotaxane-dipeptide conjugates on digested peptide uptake via intestinal human peptide transporter. *Bioconjug. Chem.* **13**, 582–587 (2002).
37. Dan, K. & Ghosh, S. One-pot synthesis of an acid-labile amphiphilic triblock copolymer and its pH-responsive vesicular assembly. *Angew. Chem. Int. Ed.* **52**, 7300–7305 (2013).
38. Tamura, A. & Yui, N. A supramolecular endosomal escape approach for enhancing gene silencing of siRNA using acid-degradable cationic polyrotaxanes. *J. Mater. Chem. B* **1**, 3535–3544 (2013).
39. Liu, R. *et al.* pH-Responsive nanogated ensemble based on gold-capped mesoporous silica through an acid-labile acetal linker. *J. Am. Chem. Soc.* **132**, 1500–1501 (2010).
40. Lange, Y., Ye, J., Rigney, M. & Steck, T. L. Regulation of endoplasmic reticulum cholesterol by plasma membrane cholesterol. *J. Lipid Res.* **40**, 2264–2270 (1999).
41. Lange, Y., Ye, J., Rigney, M. & Steck, T. L. Dynamics of lysosomal cholesterol in Niemann-Pick type C and normal human fibroblasts. *J. Lipid Res.* **43**, 198–204 (2002).
42. Lange, Y., Ye, J., Rigney, M. & Steck, T. L. Cholesterol movement in Niemann-Pick type C cells and in cells treated with amphiphiles. *J. Biol. Chem.* **275**, 17468–17475 (2000).
43. Chang, T.-Y., Chang, C. C., Ohgami, N. & Yamauchi, Y. Cholesterol sensing, trafficking, and esterification. *Annu. Rev. Cell. Dev. Biol.* **22**, 129–157 (2006).
44. Brown, M. S. & Goldstein, J. L. The SREBP pathway: regulation of cholesterol metabolism by proteolysis of a membrane-bound transcription factor. *Cell* **89**, 331–340 (1997).
45. Mbua, N. E. *et al.* Abnormal accumulation and recycling of glycoproteins visualized in Niemann-Pick type C cells using the chemical reporter strategy. *Proc. Natl. Acad. Sci. USA* **110**, 10207–10212 (2013).
46. Yokoyama, N., Seo, J.-H., Tamura, A., Sasaki, Y. & Yui, N. Tailoring the supramolecular structure of aminated polyrotaxanes toward enhanced cellular internalization. *Macromol. Biosci.* in press; DOI:10.1002/mabi.201300198.
47. Mellman, I., Fuchs, R. & Helenius, A. Acidification of the endocytic and exocytic pathways. *Annu. Rev. Biochem.* **55**, 663–700 (1986).
48. Arunachalam, B., Phan, U. T., Geuze, H. J. & Cresswell, P. Enzymatic reduction of disulfide bonds in lysosomes: characterization of a gamma-interferon-inducible lysosomal thiol reductase (GILT). *Proc. Natl. Acad. Sci. USA* **97**, 745–750 (2000).
49. Abi-Mosleh, L., Infante, R. E., Radhakrishnan, A., Goldstein, J. L. & Brown, M. S. Cyclodextrin overcomes deficient lysosome-to-endoplasmic reticulum transport of cholesterol in Niemann-Pick type C cells. *Proc. Natl. Acad. Sci. USA* **106**, 19316–19321 (2009).
50. Nakamuta, M. *et al.* Impact of cholesterol metabolism and the LXRα-SREBP-1c pathway on nonalcoholic fatty liver disease. *Int. J. Mol. Med.* **23**, 603–608 (2009).

Acknowledgments

This work was financially supported by the Grant-in-Aid for Scientific Research (No. 23107004) on Innovative Areas "Nanomedicine Molecular Science" (No. 2306) (N.Y.) from the Ministry of Education, Culture, Sports, Science, and Technology (MEXT) of Japan and The Mochida Memorial Foundation for Medical and Pharmaceutical Research (A.T.).

Author contributions

A.T. and N.Y. were involved in the design of experiments. A.T. performed the experiments and analyzed results. A.T. and N.Y. wrote the manuscript. N.Y. supervised the project. All authors discussed the results and commented on the manuscript.

Additional information

Supplementary information accompanies this paper at http://www.nature.com/scientificreports

Competing financial interests: The authors declare no competing financial interests.

How to cite this article: Tamura, A. & Yui, N. Lysosomal-specific Cholesterol Reduction by Biocleavable Polyrotaxanes for Ameliorating Niemann-Pick Type C Disease. *Sci. Rep.* **4**, 4356; DOI:10.1038/srep04356 (2014).